Modelling of the erosion / deposition pattern on the Toroidal Pumped Limiter of Tore Supra

S. Panayotis[1], D. Borodin[2], A. Kirschner[2], B. Pégourié[1],
J. Gunn[1], Y. Marandet[3], P. Monier-Garbet[1]
[1] *CEA, IRFM, F-13108 Saint Paul lez Durance, France*
[2] *Institut für Energie und Klimaforschung - Plasmaphysik, Forschungszentrum Jülich GmbH, Association EURATOM-FZJ, Trilateral Euregio Cluster, D-52425 Jülich, Germany*
[3] *Aix-Marseille Université, CNRS, PIIM, UMR 7345, F-13397 Marseille Cedex 20, France*

Wall component lifetime and retention of radioactive tritium are major concerns for next step fusion devices. Very large heat loads and particle fluxes are expected on the plasma facing components (PFCs). They lead to erosion, which limits the PFC lifetime and degrade the plasma performance due to fuel dilution and / or core radiation. Erosion and eroded material migration is also related to fuel retention by means of implantation and / or co-deposition. Different tools have been developed, aiming at understanding and modelling impurity production, transport and deposition [1,2]. Among them, the ERO code is a 3D local impurity transport and plasma-surface interaction code [2]. In this work, the ERO version initially developed for ITER blanket modules is used [3]. In the frame of the DITS campaign (Deuterium Inventory in Tore Supra [4]), a unique opportunity for broad-scale experimental validation is offered in Tore Supra. A full sector (20° in the toroidal direction) of the Toroidal Pumped Limiter (TPL, Fig. 1) was dismantled after 6 years of plasma operation and extensively studied by means of confocal microscopy, electron microscopy and lock-in thermography. This yielded a micron-scale mapping of the whole sector surface [5]. Combined with spectroscopic measurements [6], a global carbon balance was established showing that a carbon particle leaving the TPL has 50 % chances to be deposited in a TPL loaded zone, 25 % chances to build deposits in a TPL shadowed zone and 25 % chances to be deposited on another PFC, farther in the vacuum chamber [7].

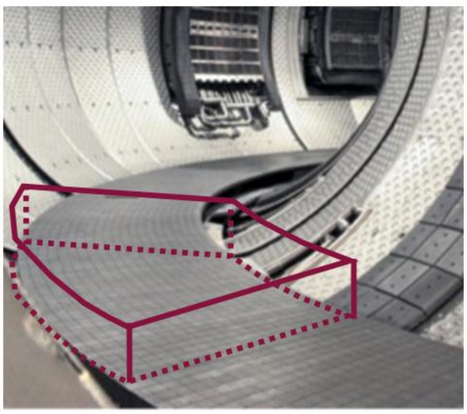

Figure 1: Picture of the vacuum vessel of Tore Supra, showing the Toroidal Pumped Limiter (TPL), and the ERO simulation box.

The Tore Supra magnetic configuration is characterized by a ripple of up to 7 % (18 coils) at the outer plasma edge, which creates a periodic footprint of the plasma on the TPL. The latter shows a periodic structure made of pairs of erosion and deposition zones, symmetrically located on both sides of the Last Closed Flux Surface (LCFS) contact point, Fig. 2a. Erosion zones are directly exposed to the plasma outflux, and probe measurements are available for the ion and electron temperatures and density. The plasma parameters were averaged for the TPL exposure period 2002-2007 (39h of cumulated plasma time), yielding $n_e(\text{LCFS}) \sim 5\times10^{18}$ m^{-3}, with an *e*-folding length $\lambda_n \sim 7$ cm, $T_e(\text{LCFS}) \sim 30$ eV, $T_i(\text{LCFS}) \sim 90$ eV and $\lambda_T \sim 6$ cm. Conversely, in the self-shadowed deposition zones no measurements are available, except the total heat flux obtained through the analysis of the Infra-Red emission of the TPL surface (Fig. 2b). An accurate mapping of the TPL sector [5] shows, for the same period, a maximum deposit thickness of ~500 μm, and a maximum erosion up to ~800 μm, corresponding to an erosion rate of ~5.5 nm/s (Fig. 2c). During discharges, the λ=426 nm CII line intensity is recorded for monitoring the carbon gross erosion, as displayed in Fig. 2d. A characteristic feature of the TPL erosion / deposition pattern is the simultaneous presence of high heat flux and significant deposition close to the LCFS contact point, as seen from the comparison of Fig. 2b and 2c.

Simulations were performed with the 3D ERO code for a full TPL sector (20° in the toroidal direction). The size of the simulation box (see fig. 1) is 93×48×10 cm^3 in the toroidal, poloidal, and vertical directions, respectively. An exact toroidal shape is used for the TPL (surface castellation structure is not considered), with a realistic magnetic configuration. In the loaded zones (Fig. 2e), characterized by long connection lengths: $L_c \sim \pi q R \sim 46$ m, the plasma parameters are taken from probe measurements. In the shadowed regions, where $L_c < 1$ m, different assumptions are used, from a total absence of plasma to the highest density and temperatures compatible with the measured heat flux. However, the heat flux distribution resulting from a basic 2D Scrape-Off Layer (SOL) calculation does not reproduce the experimental pattern, particularly the peaking close to the contact point (see Fig. 2b). For a better agreement, a perpendicular component, attributed to the funnelling effect [8], is added, with a relative contribution from 0 to 10 %. A reasonable compromise between probe and Infra-Red measurements is obtained for a relative contribution of ~5 % (Fig 2f). The incident particle flux is assumed to be dominated by D^+ ions, with an impurity concentration of C^{4+} ions varied from 0 to 5 %. ERO simulates physical and chemical (by Roth formula) erosion of the TPL material and previously built deposits, the transport of the eroded impurities in the plasma, including the effect of molecular and atomic physics, electromagnetic, friction and thermal forces and cross-field diffusion (with an effective diffusion coefficient D=3 m^2/s).

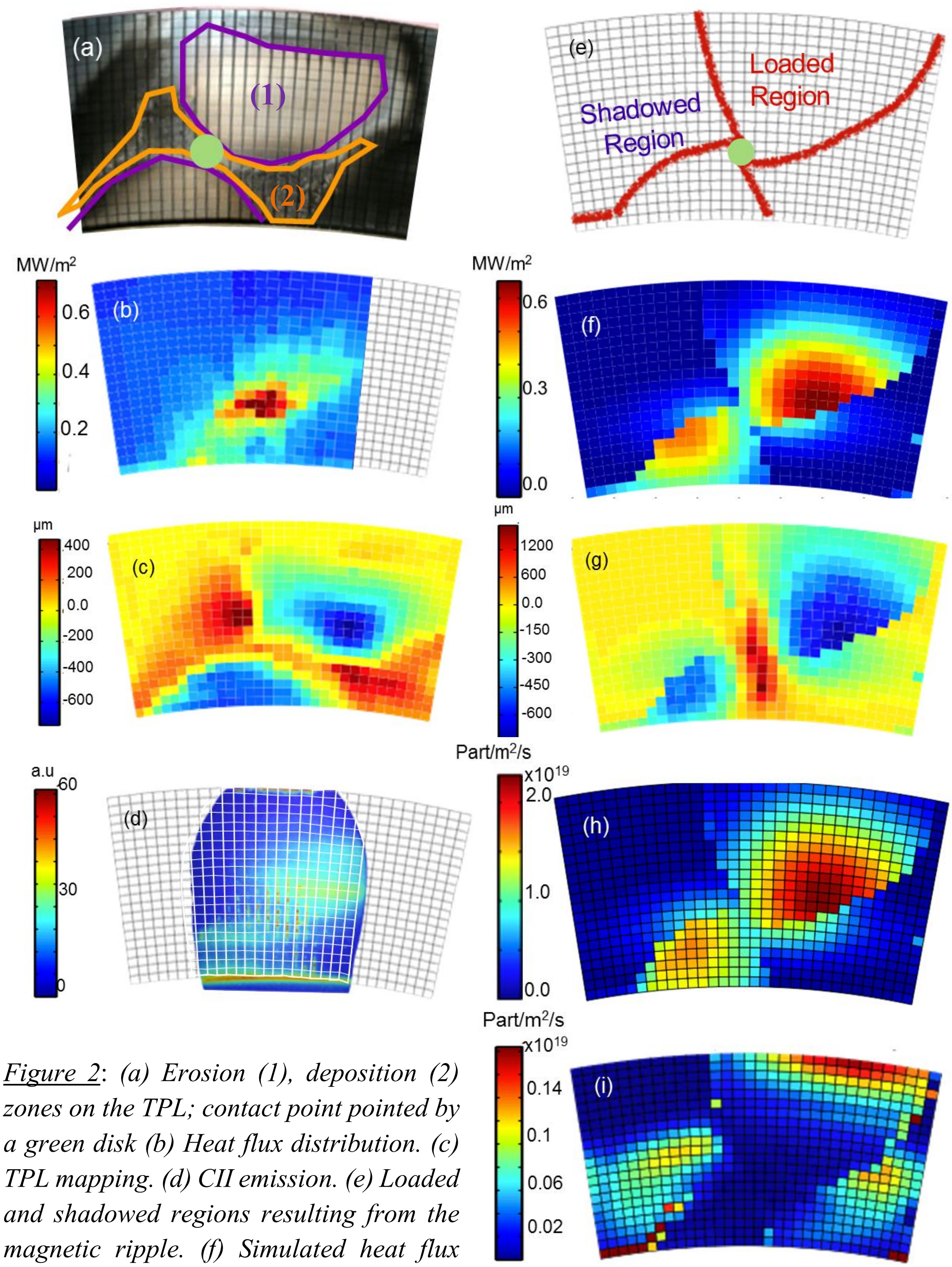

Figure 2: (a) Erosion (1), deposition (2) zones on the TPL; contact point pointed by a green disk (b) Heat flux distribution. (c) TPL mapping. (d) CII emission. (e) Loaded and shadowed regions resulting from the magnetic ripple. (f) Simulated heat flux distribution. (g) Simulated TPL-erosion / deposition pattern. (h) and (i) Physical and chemical erosion, respectively.(f)-(i) are simulated by ERO.

The modelled global carbon balance (net / gross erosion, TPL deposition / total deposition) varies with the background carbon concentration, but the distribution of the deposits on the TPL is robust with respect the flux distribution in shadowed regions (in the limits of measurements), sticking probability of hydrocarbons, deposits enhanced-erosion with respect to original material (from 1 to 5) or background carbon concentration. Simulation results displayed in Fig. 2g-2i are obtained with 18 % of flux in the shadowed zones, a reflection probability calculated by TRIM [9] for $C^{(n+)}$ and set to 0.1 for hydrocarbon ions and 1 for radicals, assuming no enhanced erosion of the deposits and no carbon in the plasma. The calculated erosion / deposition pattern is shown in Fig. 2g. Deposits are concentrated along the tangency line of the magnetic field. Two maxima are seen, on both sides of the LCFS contact point, but they are closer and sharper than on the experimental mapping (Fig. 2c). Global carbon balance indicates that a carbon leaving the TPL would have 50 % chances to be re-deposited in an erosion zone, 10 % chances to build deposits on the TPL and 40 % chances to escape the simulation box (experimental values are 50 %, 25 % and 25 %, respectively). The resulting averaged erosion rate is ~4 nm/s, in reasonable agreement with the measurements (~5.5 nm/s). The carbon gross erosion dominated by the physical sputtering (Fig. 2h), is in agreement with the CII emission distribution (Fig. 2d). The chemical sputtering dominates in the far SOL and shadowed zones, the latter contributing only ~10 % to the total (3 times lower than the experimental value [10]).

Whereas the erosion distribution and rate are fairly well simulated by ERO, the deposition pattern is not fully reproduced : the total deposition is on the TPL is 2 to 3 times smaller than in the experiments, and the migration of deposits in shadowed regions is also underestimated. One explanation might be that an eroded particle have to escape the simulation box is overestimated. Using periodic boundary conditions in the toroidal direction might allow to overcome this model shortcoming. Other improvements, planned in a near future, are a more accurate description of the CX flux (~1/3 of the particle flux) and the evolution of the deposit temperature with increasing thickness.

[1] J.N. Brooks, Fusion Eng. Des. **60** (2002) 515
[2] A. Kirschner *et al.*, Nucl. Fus. **40** (2000) 989
[3] D. Borodin et al., Phys. Scr. (2011) 014008
[4] B. Pégourié *et al.*, J. Nucl. Mater. **390-391** (2009) 550
[5] C. Martin *et al.*, J. Nucl. Mater. **438** (2013) S771
[6] Y. Marandet *et al.*, J. Nucl. Mater. **415** (2011) S157
[7] B. Pégourié *et al.*, J. Nucl. Mater. **438** (2013) S120
[8] P. Stangeby *et al.*, Nucl. Fus. **32** (1992) 2079
[9] W. Eckstein, Springer-Verlag, Berlin (1991)
[10] E. Delchambre *et al.*, J. Nucl. Mater. **390-391** (2009)